Strong Motion Site Effects in the Athens, 1999 Earthquake

Dominic Assimaki,[a] and Eduardo Kausel [b]

During the 1999 Athens Earthquake, the town of Adàmes, located on the eastern side of the Kifissos river canyon, experienced unexpectedly heavy damage. Despite the significant amplification potential of the slope geometry, topography effects cannot alone explain the uneven damage distribution within a 300m zone behind the crest, characterized by a rather uniform structural quality. This paper illustrates the important role of soil stratigraphy, material heterogeneity and soil-structure interaction on the formulation of surface ground motion. For this purpose, we first perform elastic two-dimensional wave propagation analyses based on available local geotechnical and seismological data, and validate our results by comparison with aftershock recordings. Next, we conduct nonlinear time-domain simulations that include spatial variability of soil properties and soil-structure interaction effects, to reveal their *additive* contribution in the topographic motion aggravation.

INTRODUCTION

It has been long recognized that topography can significantly affect the amplitude and frequency characteristics of ground motion during seismic events. In the recent past, documented observations from destructive seismic events show that buildings located at the tops of hills, ridges and canyons, suffer more intense damage than those located at the base: the Lambesc Earthquake [France 1909], the San Fernando Earthquake [1971], the Friuli Earthquake, [Italy 1976], the Irpinia Earthquake [Italy, 1980], the Chile Earthquake [1985], the Whittier Narrows Earthquake [1987], the "Eje-Cafetero" Earthquake [Colombia, 1998] and recent earthquakes in Greece [Kozani, 1995 and Athens, 1999] and Turkey [Bingöl,

a) Post-Doctoral Researcher, Institute for Crustal Studies, 1140 Girvetz Hall, University of California, Santa Barbara CA93106-1100
b) Professor MIT, Massachusetts Institute of Technology, Rm. 1-239, 77 Massachusetts Avenue, Cambridge MA02139

2003] are only some examples of catastrophic events, during which severe structural damage has been reported on hilltops or close to steep slopes.

Still nowadays, topographic amplification is poorly understood and the insufficient number of documented evidence prevents these effects from being incorporated in most seismic code provisions and microzonation studies, despite their undisputable significance in engineering practice. Instrumental studies that have been performed in recent years verify the macroseismic observations, by predicting systematic amplification of seismic motion over convex topographies such as hills and ridges, de-amplification over concave topographic features such as canyons and hill toes, and complex amplification and de-amplification patterns on hill slopes. The problem of scattering and diffraction of seismic waves by topographical irregularities has been also studied by many authors. The majority of these studies focus on two-dimensional simulations in which the topographic asperities are treated as isolated ridges or depressions, usually on the surface of homogeneous elastic media. Comparison between instrumental and theoretical results reveals that there is indeed qualitative agreement between theory and observations on topography effects. Nevertheless, from a quantitative viewpoint, there still exists clear discrepancy in numerous cases, where the observed amplifications are significantly larger than the theoretical predictions. Furthermore, results from instrumental studies on weak motion data or ambient noise may not be applicable to describe topography effects for strong ground shaking, which is usually associated with inelastic soil response. Indeed, there exist very few –if any– well documented case studies where topography effects are illustrated for strong ground motion.

In this paper, we use a case-study from the Athens 1999 earthquake to illustrate the decisive role of local stratigraphy, material heterogeneity and soil-structure interaction in altering the energy focusing mechanism at the vertex of convex topographies. The effects of local soil conditions are validated by comparison with weak motion data. The effects of nonlinear soil behavior and soil-structure interaction are then illustrated for the strong motion recordings. Combining our investigation with published theoretical and numerical studies, we finally propose guidelines for the estimation of topographic aggravation factors.

LOCAL SITE CONDITIONS AND STRONG MOTION RECORDS

The M_s 5.9 event that shook Athens has been characterized as the worst natural disaster in the modern history of Greece. This moderate event had a major socio-economical impact,

resulting in the loss of 150 lives, the collapse of 200 residential and industrial buildings and the severe damage of another 13,000. The location of the ruptured fault and the geography of the heavily damaged region, are schematically illustrated in Fig. 1a. Also shown on the same Figure are the locations of the four accelerograph stations, which recorded the strongest motions: KEDE, MNSA, SGMA and SPLB. One of the most heavily damaged areas was the small community of Adàmes, located next to the deepest canyon of Kifissos river, the main river of the Athens metropolitan area. The majority of local buildings comprise 2- to 4-storey concrete reinforced structures of rather uniform quality. Nonetheless, the MMI in the 1200m long and 300m wide town ranged from VIII to IX^{+}, despite its 8-10km distance from the projection of the causative fault. The location of the town next to the crest of the canyon along with the high damage intensity (as opposed to numerous other towns located at equal or smaller distances from the source where MMI did not exceed a mere VII) brought forward topography effects to justify the macroseismic observations. Behind the crest however, damage was bilaterally non-uniform, and was concentrated in two zones parallel to the river axis: one next to the crest and one at a distance about 200m-300m from it (Fig. 1b). Some scattered -yet less intense- damage was observed at intermediate locations.

A topographic survey of the canyon produced the cross-section shown in Fig. 2a. The slightly idealized geometry of the canyon used in our investigation is also shown in this figure. Note the 40m deep and the nearly 2:1 (horizontal to vertical) slope of the canyon cliff.

Geotechnical investigations of the area comprised Standard Penetration Blow Count (N_{SPT}) and cross-hole measurements. Fig. 2b illustrates the low-strain shear wave velocity profiles for three characteristic locations in Adàmes, referred to in the ensuing as profiles A, B and C. The approximate average velocity, $V_{s,30}$ of the 30m surface soil layers for the three profiles are: 500 m/sec for profile A, 400 m/sec for profile B and 340 m/sec for profile C, indicative of very stiff (profile A), just stiff (profile B), and moderately stiff (profile C) soil formations according to the European Seismic Code (EC8).

Fifteen strong-motion accelerograph stations were triggered by the main shock within 25 km from the causative fault, recording peak ground accelerations (PGA) ranging from about 0.05 g up to 0.50 g. Their location is depicted in Fig. 1a. Since no recordings were obtained in the meizoseismal area, these strong motion time-histories were used in our simulations. It should be noted, however, that these motions were recorded within a 10 km distance from the end of the ruptured zone, in a direction *perpendicular* to it, whilst -by contrast- the Kifissos

river canyon lies in front of the rupture zone. There is, therefore, strong indication that *forward-rupture directivity* effects must have been present in ground motions experienced by the town of Adàmes. To account for such near fault effects, we also used two historic time-histories from the 1966 M_s 5.6 Parkfield, CA Earthquake, which encompass long-period and high-amplitude characteristics. The response spectra of these six acceleration time histories are plotted in Fig. 3.

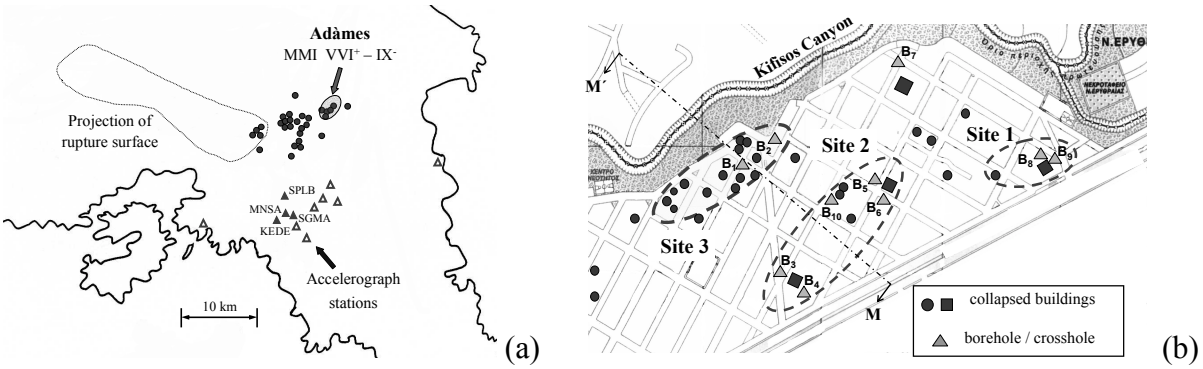

Figure 1. (a) Sketch of the map of the earthquake stricken region (the dots indicate the location of the 30 collapsed buildings with human casualties). (b) Plan view of Adàmes, showing the heavily damaged and collapsed residential (circles) and industrial (squares) buildings. Also shown are the locations of the geotechnical boreholes (B_1 - B_{10}) and the topographic cross section M-M′.

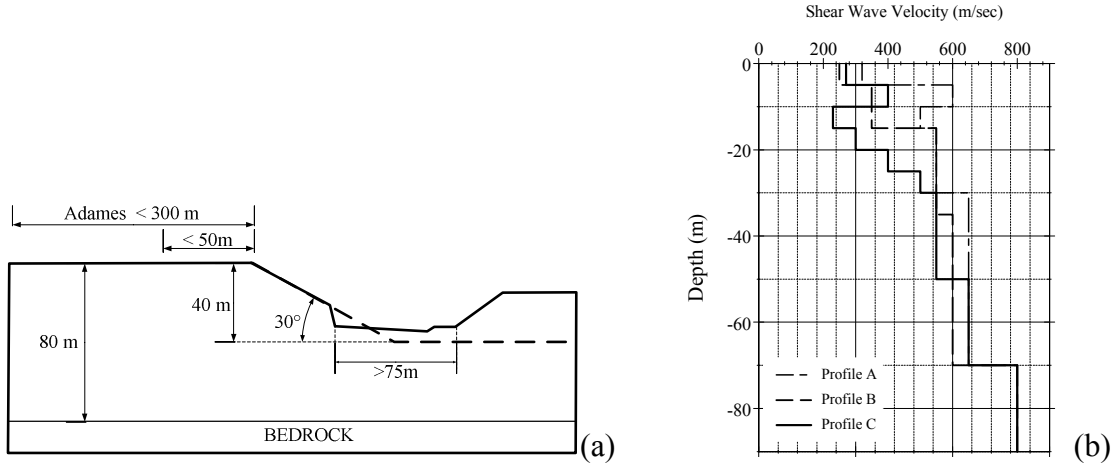

Figure 2. (a) Topography (cross-section M-M′ of the Kifissos river canyon indicated in Fig. 1b), and (b) soil conditions (shear wave velocity variation with depth of three characteristic soil profiles in Adàmes)

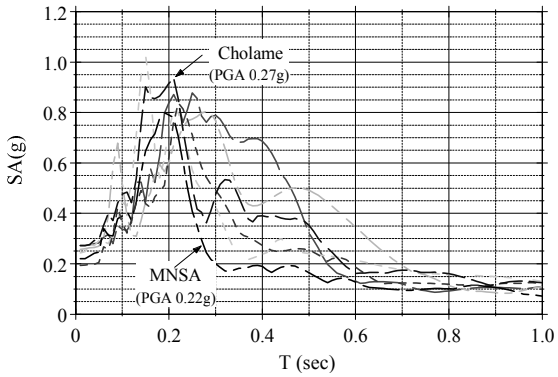

Figure 3. Acceleration response spectra of strong-motion recordings, defined at rock-outcropping in our simulations

ELASTIC SIMULATIONS

We here investigate the role of topography, soil stratigraphy and material heterogeneity by means of elastic finite-element parametric simulations. Successively, topographic aggravation factors computed for the local site conditions in Adàmes are validated by comparison with aftershock recordings from the Athens event. Simply considering the elastic response of the canyon, we can show that the site conditions in Adàmes favor a *detrimental diffraction potential*. Fig. 4 illustrates the wavefield generated by a cliff with the geometry of the Kifissos canyon, at the surface of a homogeneous halfspace upon the incidence of vertically propagating Ricker SV-waves. The direct/diffracted wavefield comprises the following waveforms: (i) Direct SV waves (denoted SV), (ii) forward and backward scattered Rayleigh waves (denoted R1 and R2 respectively) generated at the boundaries of the shadow / illuminated zone at the lower corner of the cliff, and (iii) surface waves (denoted SP) generated along the cliff, since the slope inclination of the Kifissos canyon (i = 30^o) almost coincides with the critical angle for Poisson's ratio ν=0.35 used in our simulations ($\theta_{cr} \approx 29^o$). As a result of the later, a large fraction of the incident energy is transformed into surface waves along the slope, which constructively interfere with direct SV waves behind the crest and cause excess ground motion aggravation. Note also that the surface response contains a parasitic (vertical) acceleration component in addition to the primary horizontal, which corresponds to the vertical particle motion of surface diffracted waves and is shown to carry significant portion of the seismic wave energy. For a cliff-type topographic feature on the surface of a homogeneous halfspace, our results can be summarized as follows:

1. Topographic aggravation phenomena are frequency-dependent. In particular, the location of peak acceleration (both horizontal and vertical) is controlled by the

dominant incident wavelengths, and the amplitude of peak acceleration at this location increases almost linearly with frequency. This implies that stronger aggravation is observed for higher frequency components, yet within a narrower zone behind the crest.

2. Significant differential motion is observed both behind the crest and along the slope, where transition occurs between the convex and concave part of the topography. The distance between local minima and maxima is also controlled by the dominant incident wavelengths.

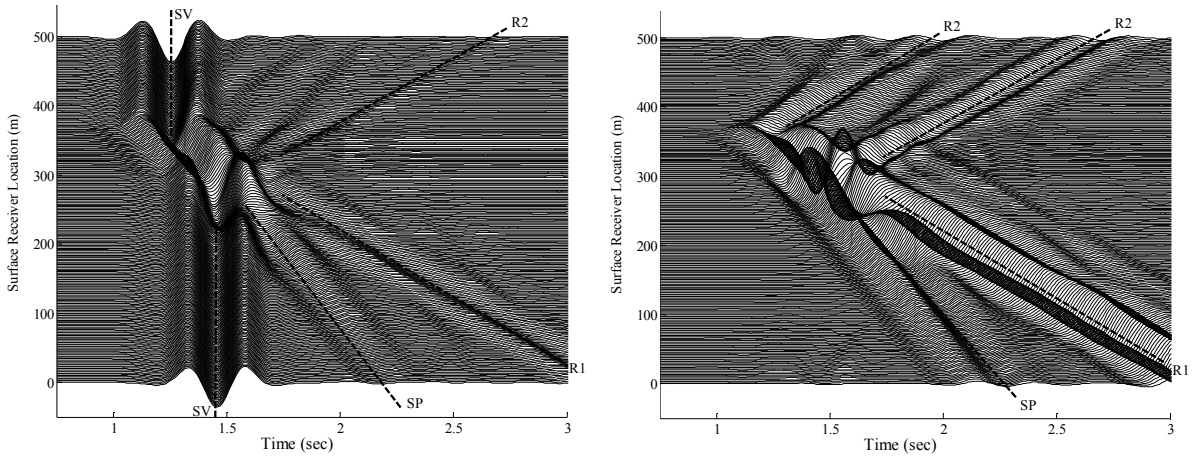

Figure 4. Synthetics of horizontal (top) and vertical (bottom) acceleration surface response, for a cliff with 30^o slope subjected to vertically propagating SV Ricker waves.

Our simulations for a homogeneous layer overlying elastic halfspace show that the bedrock-soil impedance ratio, which controls the seismic energy *trapped* in the surface layer, introduces additional complexity to the observed wavefield. Resonance of the shallow (in front of the toe) or deep (behind the crest) far-field soil columns not only controls the overall response of the configuration, but indeed enhances the topographic aggravation of motion by altering the diffraction mechanism. Similar effects are observed for a two-layered configuration, where the thickness of the surface soil layer is smaller than the height of the cliff. Results are shown in Fig. 5 for a soft layer with $V_{s1}/V_s = 0.5$ (where V_s is the shear wave velocity of the halfspace) and for thickness $h_1/h = 0.25$ (where h is the height of the cliff). Its response is compared to the homogeneous halfspace case. In summary:

1. The incident wave energy is trapped within the surface layer, and multiple reflections interact with surface waves that originate from the lower corner of the slope and propagate uphill. As a result, excess aggravation can be identified both in the time and frequency domain characteristics of the surface response.

2. The vertical acceleration component is remarkably enhanced. This effect is prominent for incident waves with wavelengths short enough to *see* the surface layer. In this case, the vertical acceleration is shown to attain amplitudes 25% larger than the corresponding response at the far-field.

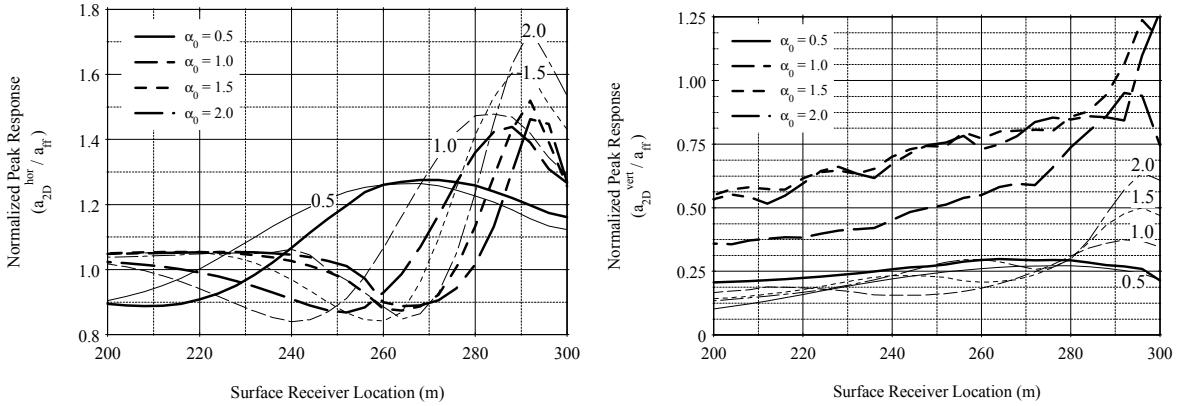

Figure 5. Normalized peak surface acceleration behind the crest for a soft surface layer with $V_{s1} / V_s = 0.5$ and $h_1 / h = 0.25$, as a function of the dimensionless frequency α_0.

We next investigate the effects of material heterogeneity. For this purpose, we generate Gaussian shear wave velocity stochastic fields using the *exponential decaying* spectral density function. Separate correlation structures are assigned to the horizontal and vertical direction to account for the mechanisms of sediment deposition. The random fields are generated in the wavenumber domain and successively denormalized and mapped on deterministic finite element models. The effects of correlation distance of the simulated random media, expressed as a function of the propagating wavelengths, are then evaluated by means of Monte Carlo simulations.

Comparison of time and frequency-domain results with the corresponding response of a homogeneous halfspace with the same background stiffness, illustrates phenomenological attenuation due to scattering for long wavelengths, and enhancement of frequency components whose wavelengths are comparable with the horizontal correlation distance of the random medium. In addition, multiple wave reflections at the localized material heterogeneities significantly increase the duration of the surface response. Fig. 6 illustrates the Fourier amplitude surface of the response behind the crest, for a typical realization of the stochastic field with $\theta_z / \lambda_0 = 0.0625$ and $\theta_x / \lambda_0 = 0.625$, where θ_i is the correlation distance in the i^{th} direction and λ_0 is the dominant propagating wavelength. Clearly, the erratic frequency content of the response and the amplification level of high frequency components cannot be simulated by means of a homogeneous medium.

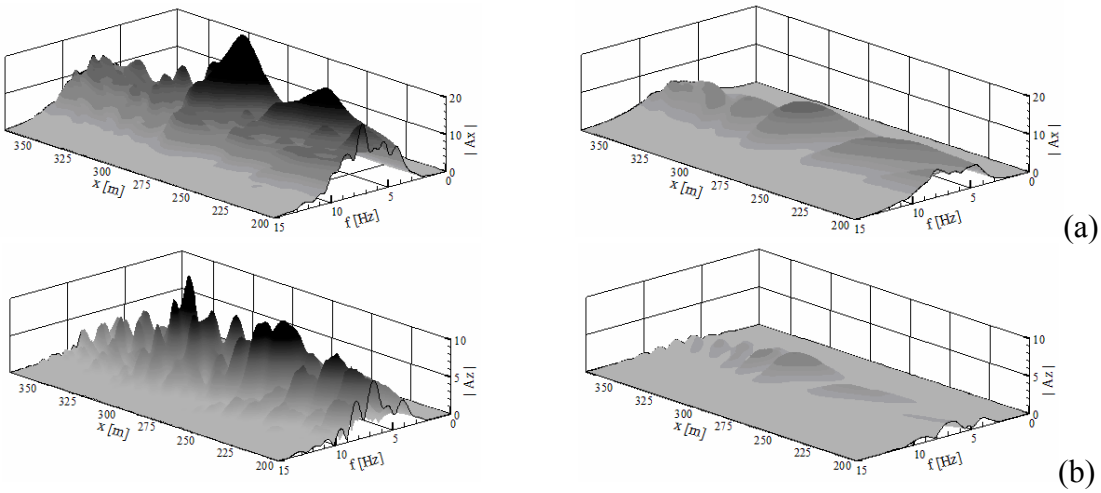

Figure 6. Fourier amplitude surface of (a) horizontal and (b) vertical response, for random field with $\theta_z/\lambda_0 = 0.0625$ and $\theta_x / \lambda_0 = 0.625$ (left) and homogeneous halfspace (right) with the same background shear wave velocity.

LOCAL SITE CONDITIONS AND RECORDED FIELD EVIDENCE

The 2D response of the stratified soil configurations corresponding to profiles A, B and C is next evaluated by means of elastic simulations. The numerical model is now subjected to the strong motion time-histories described above, and results of our analyses can be summarized as follows:

1. For the broad-band seismic input, topographic aggravation occurs within a zone behind the crest, approximately equal to the width of the topographic irregularity (L = 70m). This is found to be in accordance with results of our parametric investigation.

2. Two-dimensional aggravation of the horizontal response is shown to be rather *insensitive* to soil stratigraphy, yet enhanced in comparison to the homogeneous halfspace case. Peak amplification is of the order of 30% a_{ff}, where a_{ff} is the far-field peak surface acceleration.

3. The magnitude of parasitic acceleration however, shows strong dependence on the soil stratigraphy. This effect is primarily controlled by stiffness of the surface layer. In particular, results show that the amplitude of the vertical acceleration range from 0.25aff for the stiffer profile A to 0.70aff for the softer profile C.

Significant corroboration of our elastic numerical simulations comes from two sets of ground motions, recorded during two aftershocks of the Athens 1999 event. The instruments were installed in the free field, two at a site x ≈ 300m from the crest, and one at x ≈ 10m from

the crest. The two major aftershocks have provided the empirical transfer function spectra that are plotted in Fig. 7. Successively, class-A predictions of the elastic response of the configuration were obtained for 20 realizations of the stochastic field; the mean and standard deviation of the numerically predicted transfer functions are also shown in Fig. 7. It can readily be seen that the recorded and computed results are in very good agreement, offering strong support to our conclusions.

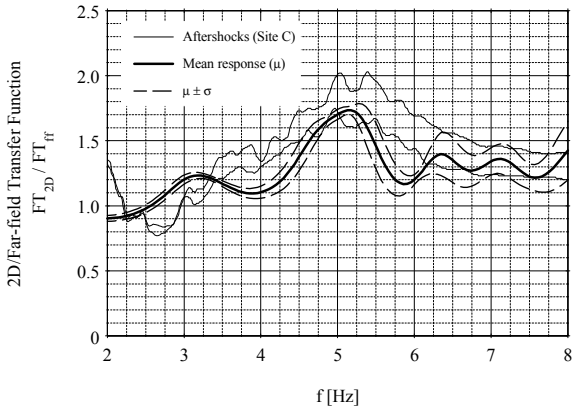

Figure 7. 2D/Far-field empirical transfer function from the records of two strong aftershocks, and comparison with numerical results of 20 Gaussian stochastic field realizations

NONLINEAR SIMULATIONS

We first investigate the effect of local soil conditions by means of 1D nonlinear wave propagation analyses. The far-field profiles A, B and C are subjected to the six strong-motion time histories, and the surface response is computed in the frequency-domain using an iterative equivalent linear algorithm (Kausel & Assimaki, 2001), and in the time-domain, by incremental nonlinear finite element simulations (Hayashi *et al*, 1994). The surface response computed by means of the two approaches, is found to be in remarkable agreement.

We next perform 2D nonlinear simulations and illustrate the degree of topographic aggravation in the frequency domain by means of the response spectral ratio of the 2D horizontal acceleration component to the corresponding far-field response. We refer to this ratio as Topographic Aggravation Factor (TAF); the mean TAF at x = 20m from the crest is plotted in Fig. 8 as a function of period (T), for profile C and the ensemble of strong input motions. As can readily be seen, the elastic and equivalent linear solution yield very similar spectral amplification values, whereas the nonlinear solution shows significant enhancement of the high frequency components. In accordance to the effects of material heterogeneity, nonlinearity introduces a *strain-compatible* randomness that favors amplification of short

wavelength components. Amplification of high-frequencies is even more pronounced when material heterogeneity (*small-strain* randomness) is also modeled in our simulations.

The spatial distribution of peak surface response is shown in Fig. 9 for profile C. The erratic surface response, that is substantially amplified and more confined in the vicinity of the crest, is consistent with the enhancement of high-frequencies. From the ensemble of our simulations, strong-motion site effects in Adàmes can be summarized as follows:

1. Profile A being the stiffest of the three sites, shows an appreciable degree of soil amplification. However, soil amplification does not alone suffice to explain the observations. Topography and local soil conditions have equally aggravated the motion intensity by approximately 30%; this justifies the observed damage distribution, which was moderate and more intense next to the crest. In fact, for the very stiff and relatively homogeneous profile, the moderate damage intensity can be even justified by means of elastic 2D simulations.

2. Profile B is softer than profile A, and simulations show larger amplification over a wider period range (as high as 60%). The fundamental period of the far-field nearly coincides with the dominant period of seismic excitation, indicating the decisive role of soil conditions. This is further verified by the damage intensity distribution, nearly homogeneous within the 300m zone behind the crest.

3. Profile C is the softest of the three sites and is characterized by a rather distinct surface soil layer. One-dimensional nonlinear simulations predict deamplification of the incident seismic motion for $T < 0.25$ sec; this effect, combined with the 30% topographic aggravation of horizontal motion cannot explain the observations for one of the most heavily damaged regions in the 7-9-99 earthquake. It is indeed the excess amplitude of vertical acceleration, namely 120% of the corresponding far-field motion, which is believed to have caused substantial damage. The intensity of the parasitic motion predicted in our nonlinear simulations cannot be approximated by means of equivalent linear analyses that yielded a marginal 40% for the same configuration.

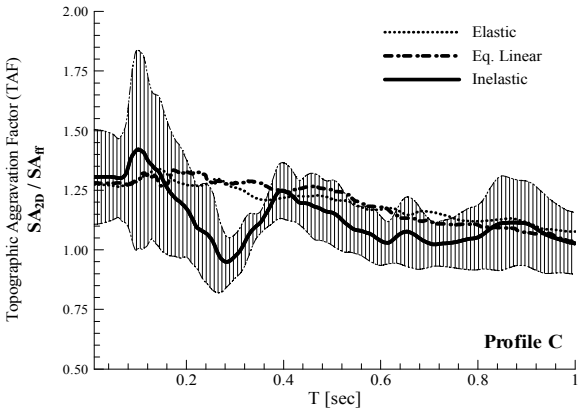

Figure 8. Mean Spectrum of Topographic Aggravation Factor at x=20m from the crest, for Profile C and six strong-motions

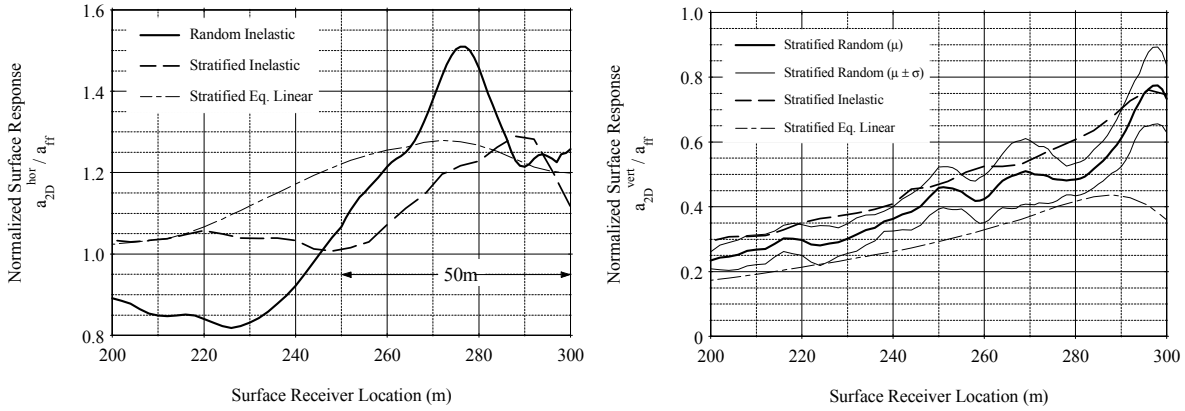

Figure 9. Mean normalized peak acceleration for Profile C and a random medium with the same mean stiffness and θ_z = 2.5m and θ_x = 16.0m, subjected to six strong-motions

NONLINEAR SOIL-STRUCTURE INTERACTION

We finally simulate the nonlinear response of a rigid surface structure founded next to the crest. A schematic illustration of the configuration is shown in Fig. 10a. For the stiff soil formations in Adàmes, altering of the response at the location of the structure is shown to be governed by kinematic interaction phenomena, namely the inability of the structure to follow the strongly differential surface response. As a result, frequency components of the horizontal response whose wavelengths are comparable or shorter than the dimensions of the structure are filtered. Nevertheless, the vertical acceleration is almost unaffected by the presence of the stiff structure and moreover, the differential surface ground motion imposes additional rocking loading. Results are shown for the stratigraphy of profile C in Fig.10b, where the spectrum of TAF at the centerline of the structure is compared to the free-field response at the same location. Note that the high-frequency components of the response are filtered, yet for higher periods, the frequency content of motion is practically unaffected by the presence

of the structure. This verifies that no material yielding occurs as a result of the structural static loading or inertial soil-structure interaction.

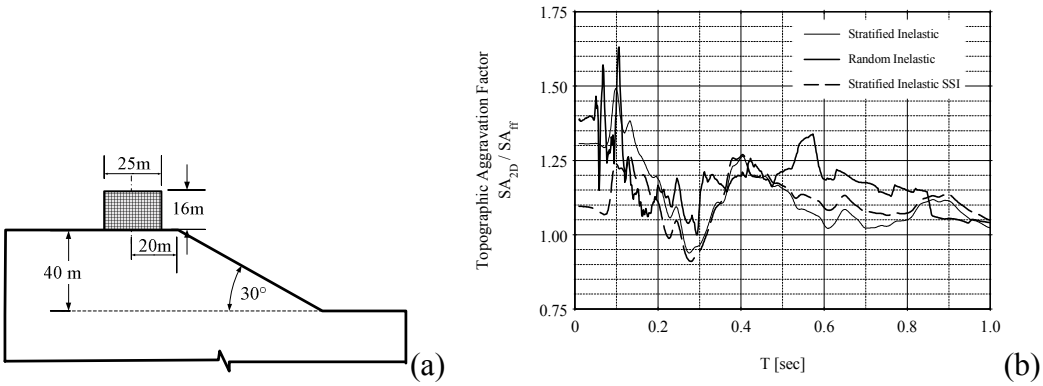

Figure 10. Schematic illustration of numerical model, and mean spectrum of Topographic Aggravation Factor at x=20m from the crest, for Profile C and six strong-motions

CONCLUSIONS

Based on a case study from the Athens 1999 Earthquake, we have illustrated the decisive role of local soil conditions and nonlinear soil behavior in the degree of topographic motion aggravation. We have shown that:

1. Nonlinear soil amplification of seismic motion can be substantial, even for typical stiff sites such as the soil profiles in Adàmes, which are characterized by average shear wave velocity 400m/s.

2. Topographic aggravation of seismic motion is a function of local soil conditions and seismic motion intensity. As a result, elastic theoretical/numerical simulations and weak motion data may not be applicable to describe topography effects for strong seismic events, especially the amplitude of high frequency components.

3. The equivalent linear method with frequency-dependent dynamic soil properties may be used to describe soil amplification for horizontally stratified media, even for weak heterogeneous formations. Nonetheless, it cannot simulate the 2D wavefield direction, and therefore cannot be used to describe the surface response of two-dimensional topographic features to strong ground motion, in terms of peak amplitude, frequency content and spatial distribution of motion.

4. The parasitic acceleration component can attain quite substantial amplitude close to the crest of cliff type topographies (on the order of magnitude of the primary far-field surface response); its amplitude is even further enhanced for the case of

heterogeneous media characterized by soft surface formations and subjected to strong seismic input. Nonetheless, our simulations for vertical seismic incidence are typical of distant seismic events; further investigation is necessary to evaluate the effects of near-source events, where the incident wavefield can be strongly inclined.

The normalization of the 2D response to the far-field allows topography effects to be quantified as a function of local soil conditions. With an adequate number of strong-motion case studies, the proposed Topographic Aggravation Spectrum can be used to estimate topographic amplification in engineering design.

REFERENCES

Ashford S.A., N. Sitar, J. Lysmer and N. Deng, 1997. Topographic Effects on the Seismic Response of Steep Slopes, *Bulletin of the Seismological Society of America*, **87**(3), pp 701-709.

Assimaki D. and G. Gazetas, 2004. Soil and topographic amplification on canyon banks and the Athens 1999 earthquake, *Journal of Earthquake Engineering*, **8**(1), pp 1-44.

Assimaki D., A. Pecker, R. Popescu and J.H. Prevost, 2003. Effects of Spatial Variability of Soil Properties on Surface Ground Motion, *Journal of Earthquake Engineering*, **7**(1), pp 1-44.

Gazetas G., P.V. Kallou and P.N. Psarropoulos, 2002. Topography and Soil Effects in the Ms 5.9 Parnitha (Athens) Earthquake: The Case of Adámes, *Natural Hazards*, **27**(1-2), pp 133-169.

Hayashi, H., M. Honda and T. Yamada, 1992. Modeling of nonlinear stress strain relations of sands for dynamic response analysis, *Proc. 3rd World Conf. on Earthquake Engineering*, (publisher) Balkema, Madrid, Spain, pp 6819-6825.

Kausel E. and D. Assimaki, 2001. Simulation of dynamic, inelastic soil behavior by means of frequency-dependent shear modulus and damping, *Journal of Engineering Mechanics*, ASCE, **128**(1), pp 34-47.

Pavlides S.B, G. Papadopoulos and A. Ganas, 2002. The Fault that Caused the Athens September 1999 Ms = 5.9 Earthquake: Field Observations, *Natural Hazards*, **27**(1-2), pp 61-84.

Popescu R., 1995. *Stochastic variability of soil properties: data analysis, digital simulation, effects on system behavior*, PhD thesis, Princeton University, Princeton, New Jersey.

Prevost J.H., 1981. DYNAFLOW: A nonlinear transient finite element analysis program, *Technical report, Department of Civil Engineering and Operations Research*, Princeton University, Princeton, New Jersey.